**ARTICLE**

# Design, synthesis and evaluation of E2-25K derived stapled peptides

Morag E. Watson[1] | Daniel Scott[2] | Craig Jamieson[1] | Robert Layfield[2] | Andrew M. Mason[3]

[1]Department of Pure and Applied Chemistry, University of Strathclyde, Glasgow, UK

[2]School of Life Sciences, University of Nottingham Medical School, Nottingham, UK

[3]Medicinal Sciences and Technology, GlaxoSmithKline Research and Development, Medicines Research Centre, Stevenage, Herts, UK

**Correspondence**
Craig Jamieson, Department of Pure and Applied Chemistry, University of Strathclyde, 295 Cathedral Street, Glasgow G1 1XL, UK
Email: craig.jamieson@strath.ac.uk

**Abstract**

Stabilised peptides are now established as potential drug candidates to probe previously intractable molecular targets, such as protein-protein interactions. Herein, we report the design and synthesis of eight short helical peptide analogues of the ubiquitin conjugating enzyme, E2-25K, as potential antagonists of the interaction between E2-25K and the Alzheimer's Disease (AD) associated ubiquitin mutant Ubb + 1. Biochemical evaluation revealed four putative antagonists of the Ubb + 1/E2-25K interaction that reduced incorporation of Ubb + 1 into polyubiquitin chains in *vitro*, validating the potential of this approach as a therapeutic strategy.

**KEYWORDS**

Alzheimer's, staples, ubiquitin

## 1 | INTRODUCTION

In Alzheimer's disease (AD) there is an urgent need for understanding disease pathomechanisms that underlie the accumulation of neurotoxic protein aggregates which represent the characteristic pathological hallmarks of the condition.[1] Improved knowledge of protein interactomes, and the physiological significance of post translational modifications has led scientists to probe the link between malfunction of important cellular regulatory processes and the onset of neurodegeneration.[2,3] Of particular interest is protein ubiquitination as part of the ubiquitin proteasome system (UPS) which mediates degradation of intracellular proteins in a non-lysosomal approach.[4] Within the UPS, excess or misfolded proteins are covalently tagged with polyubiquitin chains through a multiple enzyme ligation process. Ubiquitin (Ub) is conjugated to the E1-activating enzyme through an ATP-mediated thiol bond between the *C*-terminal Gly of Ub and a Cys

of E1. The activated Ub is then transferred to an E2-conjugating enzyme through transacylation to another Cys site on the E2. The E2-Ub complex then interacts with an E3 ligating enzyme bound with the protein marked for degradation by the UPS, transferring the Ub to a Lys residue of the target. The conjugated Ub can itself be ubiquitinated through one of its lysine residues, commonly through Lys$^{48}$ for a UPS signal, giving rise to polyubiquitin chains which chaperone the target protein into the proteasome for degradation.

It has been shown that function of the UPS could be inhibited in AD, however the mechanism(s) by which this important regulatory system is malfunctioning is incompletely understood. One such mechanism is mediated through a frameshift mutant form of ubiquitin, Ubb + 1, which has been shown to accumulate in the neurons of patients with AD,[5–8] but is absent in age matched non-disease controls.

Ubb + 1 has an primary amino acid related sequence to Ub, however, contains a *C*-terminal 19 amino acid extension, lacking the free Gly$^{76}$ essential for conjugating to UPS targets. *in vitro* and in cellulo studies in our own laboratories have shown Ubb + 1 can itself be

---

ubiquitinated, creating Ubb + 1 capped polyubiquitin chains.[9] These chains have shown resistance to de-ubiquitinating enzymes, and are capable of binding to and completely inhibiting the proteasome. Following on from this initial data, a review of subsequent literature suggests that this original hypothesis is broadly supported, and offers further insight into the age-dependent accumulation of Ubb + 1, and how Ubb + 1-mediated proteasome inhibition may contribute to Alzheimer's disease.[10]

Incorporation of Ubb + 1 into the unanchored polyubiquitin chains is mediated through the protein-protein interaction (PPI) between Ubb + 1 and the conjugating enzyme E2-25K through a Ub-binding associated domain (UBA, Figure 1).[11,12] This relatively small 400 $Å^2$ PPI could provide a novel target for AD therapeutics as it is critical for the incorporation of Ubb + 1 into polyubiquitin chains. The Ub-binding domain of E2-25K is dominated by a short α-helical motif (labelled α-9), which binds to Ubb + 1 through predominantly hydrophobic interactions of Val[120], Thr[124] and Leu[128] with the Ubb + 1 surface, and a single salt-bridge between Glu[125] and Arg[42] of E2-25K and Ubb + 1, respectively (Figure 2).

PPIs as potential drug targets have historically been difficult to target due to their large surface area which is generally devoid of pocket-like structures in which small molecules can bind.[13] Despite recent advances in identifying "hot-spots" that might serve as binding sites for small molecule inhibitors, using macromolecular constructs has proven effective in targeting various PPIs, and in particular short peptide mimics of the parent protein.[14] Pioneering work by both Grubbs and Verdine have shown that it is possible to inhibit PPIs through creating stabilised helical peptides capable of mimicking the α-helical interface at the PPI surface.[15–18] The use of stabilised peptides allows for maximum specific interactions with the target surface in the absence of any small molecule binding sites through combining the non-covalent forces and topological recognition of the parent sequence. Based on this strong precedence, we elected to employ the technique of peptide stapling for our initial studies into inhibiting the E2-25K/Ubb + 1 PPI by creating a focused palette of short helical peptide analogues of the α-9 helix of E2-25K.

## 2 | MATERIALS AND METHODS

### 2.1 | General

All reagents, resins and solvents were obtained from commercial suppliers and were used without further purification unless otherwise stated. Purified solvents were stored in a septum-sealed oven died flask over previously activated 4 Å molecular sieves, and purged and stored under $N_2$. Anhydrous THF and DCM were obtained from a PureSolv SPS-400-5 solvent purification system.[19]

### 2.2 | Solid phase peptide synthesis

Reagents used in SPPS were as follows: All Fmoc-protected amino acids were purchased from Novabiochem unless stated in the text. Rink amide MBHA resin (0.78 mmol/g loading) was purchased from Novabiochem. 1-[Bis(dimethylamino)methylene]-1H-1,2,3-triazolo[4,5-b]pyridinium 3-oxide hexafluorophosphate (HATU) and 1-Hydroxy-7-azabenzotriazole (HOAt) were purchased from Fluorochem. Triisopropyl silane (TIS), Piperidine, N-methylmorpholine (NMM) and Trifluoroacetic acid (TFA) were purchased from Alfa Aesar. Acetic anhydride, Diisopropylethylamine (DIPEA) and Bis(tricyclohexylphosphine)benzylidine ruthenium(IV) dichloride (Grubbs first generation catalyst) were purchased from Sigma-Aldrich. All solvents were purchased from Sigma-Aldrich with the exception of dimethylformamide (DMF) which was purchased from Rathburn Chemicals Ltd.

All automated couplings were carried out on a Protein Technologies, Tribute automated synthesizer.

Resin was swollen in DCM for 10 min prior to any synthesis. Deprotections were carried out using a solution of 20% piperidine in DMF (3 × 5 min). N-terminal capping was achieved using 15% acetic anhydride in DMF (3 × 5 min). All standard couplings were carried out using HATU (5 equiv.), amino acid (5 equiv.) and DIPEA (10 equiv.) in DMF. Alkene containing amino acid couplings were carried out using a Merrifield bubbler with HATU (2.5 equiv.), amino acid (2.5 equiv.) and DIPEA (5 equiv.) in DMF. N-terminal threonine couplings were
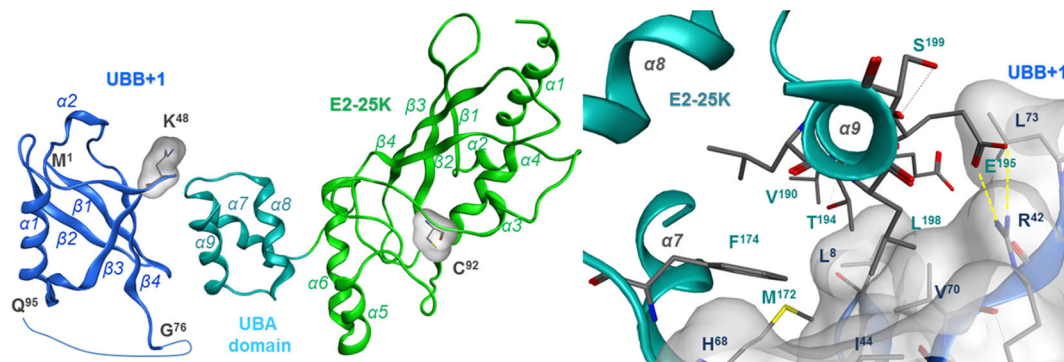


**FIGURE 1** The Ubb + 1/E2-25K proteinprotein interaction. Main interaction surface between Ubb + 1 and E2-25K coloured by domain of E2-25K. α-9 (dark purple) within the ubiquitin binding domain (UBA) dominates the PPI with some additional interactions from the loop between α-8 and α-7 of E2-25K. Crystal Structure PDB ID: 3K90

**FIGURE 2** Key interactions between Ubb + 1 (Blue) and E2-25K (Purple). Lipophilicity of Ubb + 1 demonstrated, with hydrophilic sections shown in dark blue, and lipophilic surfaces shown in lime green. The α-9 helix of E2-25K is shown in purple with key residues and their interactions highlighted. The Ubb + 1/ E2-25K PPI is dominated by hydrophobic interactions and a key salt bridge between Glu$^{125}$ of E2-25K with Arg$^{42}$ of Ubb + 1
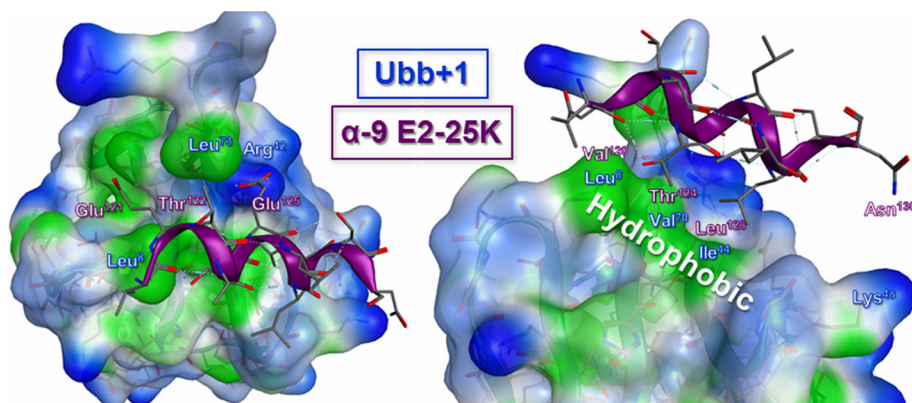


carried out using HATU (5 equiv.), HOAt (4 equiv.), amino acid (5 equiv.) and DIPEA (10 equiv.) in DMF. Coupling times varied per peptide as presented in the Supporting Information.

Ring-closing metathesis was achieved using 40 mol% Grubbs first generation catalyst in DCM (10 mM). Methathesis was complete after 3 × 2 Hr reactions under sonication.

For the synthesis of staple **8**, FmocGlu(OAllyl)OH was employed. Allyl deprotection was carried out using 4 × Pd(PPh$_3$)$_4$ (10 mol%) and PhSiH$_3$ (10 equiv.) in DCM followed by 4 × Sodium diethyldithiocarbamate trihydrate (0.8 equiv) in DMF. This was followed by HATU-mediated cyclisation to furnish the pyroglutamate analogue.

All peptides were cleaved using a mixture of TFA/TIS/H$_2$O (95:2.5:2.5) for 4 h, filtered and precipitated into Et$_2$O. Centrifugation and preparative HPLC gave the completed peptides. Reverse-phase HPLC purification of peptides was carried out using a Gilson preparative HPLC system of 322 pumps coupled to a 151 UV/Vis spectrometer, 234 Autoinjector and a GX-271 liquid handler using a Agilent Zorbax SB-C18, 21.2 × 100 mm, 5 μ column at room temperature. Purifications were performed using gradient methods ranging from 5% to 90% MeCN in H$_2$O over 30 min at a flow rate of 10 mL/min. Analysis was carried out using Gilson Trilution software.

Reverse-phase analytical HPLC analysis of peptides was carried out on an Agilent 1260 Infinity system using a Macherey Nagel, EC 250/4.6, Nucleodur C18 Gravity, 5 μm Column at room temperature. Purity was required to be ≥90% by UV at 214 nm over a gradient of 5%-95% MeCN in H$_2$O for 30 min.

## 2.3 | Circular dichroism spectroscopy

Circular Dichroism was carried out on an Applied Photophysics Chirascan plus CD spectrometer with temperature control. All samples were prepared using phosphate buffer solution (50 mM, pH 7). For 0.1 and 1 mm cells, peptides were made to a concentration of 200 and 50 μM, respectively. Machine parameters for each sample were as follows: Wavelength = 190-260 nm, Step resolution = 0.5 nm, accumulations = 10, Bandwidth = 1 nm, Temperature = 20 °C. All spectra were measured in ellipticity (mdeg) after background substraction. All curves shown are smoothed using standard parameters. Helicity calculated from mean residue ellipticity (Equation 1)

**TABLE 1** calculated maximum mean residue ellipticity at 222 nm

| Temp. (°C) | n | [θ]$_{max}$ |
|---|---|---|
| 20 | 11 | −28 364 |
| 20 | 12 | −29 250 |

divided by maximum mean residue ellipticity (Table 1) at 222 nm where T = Temp (°C) = 20 °C, n = no. of amino acids in peptide = 11, K = Correction factor = 3, C = Sample concentration (M), l = Cell path length (mm).

$$\%\text{helicity} = [\theta]_{222}/[\theta]_{max} \qquad (1)$$

where

$$[\theta]_{222} = \theta_{obs} \div (Cln); [\theta]_{max} = (-44\,000 + 250T)\left(1 - \frac{K}{n}\right)$$

## 2.4 | Peptide NMR

$^1$H, NOESY and TOCSY data were obtained at 600 MHz using aBruker Advance II+ NMR with Staple 1 diluted to 2 mM in phosphate buffer (50 mM, pH 7, 10% D$_2$O, 90% H$_2$O) and COSY data was obtained with Staple 1 diluted to 2 mM in D$_2$O. One-dimensional 1H NMR data were acquired using a Bruker excitation sculpting sequence (zgesgp) to eliminate the solvent resonance. Data was acquired at 128 scans over a frequency of 7.2 kHz (12 ppm), centred at 4.703 ppm into 32.8 K data points (acquisition time of 2.27 s) with a total spectra time of 9 min. SPARKY NMR visualisation software was used to interpret, assign and integrate all 2D spectra.[20]

## 2.5 | In *vitro* polyubiquitination assays

10× Reaction buffer stock solution contained 500 mM Tris buffer, 100 mM MgCl$_2$, 10 mM ATP, 10 mM DTT (pH 7.5). Peptides were prepared as a 300 μM stock solution in reaction buffer.

All reaction were carried out containing Ubb + 1 (50 μM), Ub (50 μM), E1 (0.1 μM), E2-25K (1 μM) and test peptide (30 μM) and made up to 50 μL with distilled water.

The reactions were incubated for 4 h at 37 °C on a shaking incubator then quenched with 20 μL of SDS-PAGE gel application buffer. The reaction solution was then split into equal 35 μL aliquots and run on a 5%-20% SDS-PAGE gradient gel. Following western transfer to nitrocellulose, one set of samples was probed vs anti-VU1 (anti-ubiquitin, 1:1000) and the other vs anti-Ubb + 1 (1:1000).
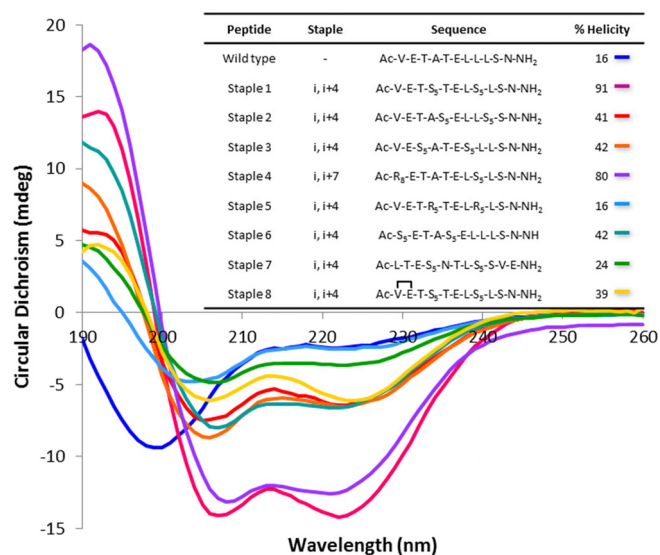
## 2.6 | Molecular modelling

Chemical Computing Group's Molecular Operating Environment (MOE) software was used to visualize, edit and compute all structures. An AMBER12:EHT force field was used for all structures.[21] Peptide models were created through modifications of the crystal structure of E2-25K in complex with Ubb + 1 (PDB ID 3K9O).[11] The structure of E2-25K was edited to only the α9 segment (Val$^{190}$ – Asn$^{200}$) and modified to each peptide structure using the "builder" function of the software. All i, i + 4 staples were assumed to be *cis* configuration and all i, i + 7 staples were assumed to be *trans* based on the study by Verdine *et al*.[17] Free peptides were energy minimised, then minimised again against the full Ubb + 1 structure.

## 3 | RESULTS AND DISCUSSION

As stated above, the current study centred around the synthesis of a focused array of stapled peptides as small helical surrogates of E2-25K. In the first instance, a control peptide which contained the 11 amino acid sequence of α-9 from wild type E2-25K with no structural constraint was prepared. A range of i, i + 4 staples were designed based on this sequence which were anticipated not to disrupt the key

hydrophobic and electrostatic interactions crucial for binding with the surface of Ubb + 1 from consideration of the available crystal structure of the complex and associated NMR data.[11] Peptide staples **1**, **2**, **3** and **6** contain the all hydrocarbon linker at differing points in the sequence, resulting the staple itself being exposed to solvent (constructs **1** and **3**) or potentially against the Ubb + 1 surface (peptides **2**, and **6**). Peptide staple **5** was examined to confirm the previous

| Peptide | Staple | Sequence | % Helicity |
|---|---|---|---|
| Wild type | - | Ac-V-E-T-A-T-E-L-L-L-S-N-NH$_2$ | 16 |
| Staple 1 | i, i+4 | Ac-V-E-T-S$_5$-T-E-L-S$_5$-L-S-N-NH$_2$ | 91 |
| Staple 2 | i, i+4 | Ac-V-E-T-A-S$_5$-E-L-L-S$_5$-S-N-NH$_2$ | 41 |
| Staple 3 | i, i+4 | Ac-V-E-S$_5$-A-T-E-S$_5$-L-L-S-N-NH$_2$ | 42 |
| Staple 4 | i, i+7 | Ac-R$_8$-E-T-A-T-E-L-S$_5$-L-S-N-NH$_2$ | 80 |
| Staple 5 | i, i+4 | Ac-V-E-T-R$_5$-T-E-L-R$_5$-L-S-N-NH$_2$ | 16 |
| Staple 6 | i, i+4 | Ac-S$_5$-E-T-A-S$_5$-E-L-L-L-S-N-NH | 42 |
| Staple 7 | i, i+4 | Ac-L-T-E-S$_5$-N-T-L-S$_5$-S-V-E-NH$_2$ | 24 |
| Staple 8 | i, i+4 | Ac-V-E-T-S$_5$-T-E-L-S$_5$-L-S-N-NH$_2$ | 39 |

**FIGURE 4** Circular Dichroism spectra of designed stapled peptides. The wild type sequence, shown in black, has no protein secondary structure exhibiting an unstructured CD spectra with a single minima at 200 nm. All other peptides exhibited a helical secondary structure, with maxima at 198 nm and minima at 208 and 222 nm. Helicity was calculated from the mean residue ellipticity at 222 nm and maximum mean residue helicity for the sequence
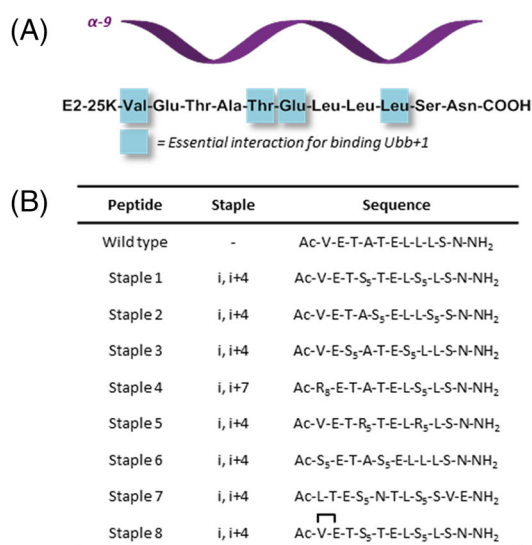
**FIGURE 3** Proposed stapled peptide analogues of α-9 of E2-25K. (A) - The α-9 helix of E2-25K consists of an 11 amino acid sequence. Residues shaded are essential for target binding with Ubb + 1. (B) Short helical peptide derived from the sequence of E2-25K were designed. Variation in staple position and length could give significant differences in peptide helicity or target affinity. (C) Model of staple 1 binding with Ubb + 1. Residues highlighted in blue correspond to those highlighted in the sequence of E2-25K deemed essential for binding with Ubb + 1

literature precedent that (R), (R) i, i + 4 staples are in general less helical in nature than their corresponding (S), (S) counterparts.[22] An i, i + 7 staple was also designed with the hydrocarbon linker towards the C-terminal end of the peptide sequence (construct 4; Figure 3).

An isomeric peptide system, staple 7, was designed in which the primary amino acid sequence of staple 1 was reorganised to determine if replacements at certain positions in the sequence could be tolerated whilst maintaining the physicochemical properties of the peptide compared to staple 1. In particular, we were interested whether Glu[6] could be substituted to a Thr and still maintain a key hydrogen-bond with Arg[42] of Ubb + 1. Finally, an N-terminal cyclised analogue of staple 1 was designed (construct 8) in which Glu[10] would be selectively deprotected on the solid phase, then cyclised onto the backbone NH of Val[11] using standard HATU chemistry (see Supporting Information for further details). It was proposed that this N-terminal cyclisation would facilitate further hydrophobic interactions with the surface of Ubb + 1 as the side chain acid of Glu[10] has no key interactions with Ubb + 1 from consideration of the available X-ray data.
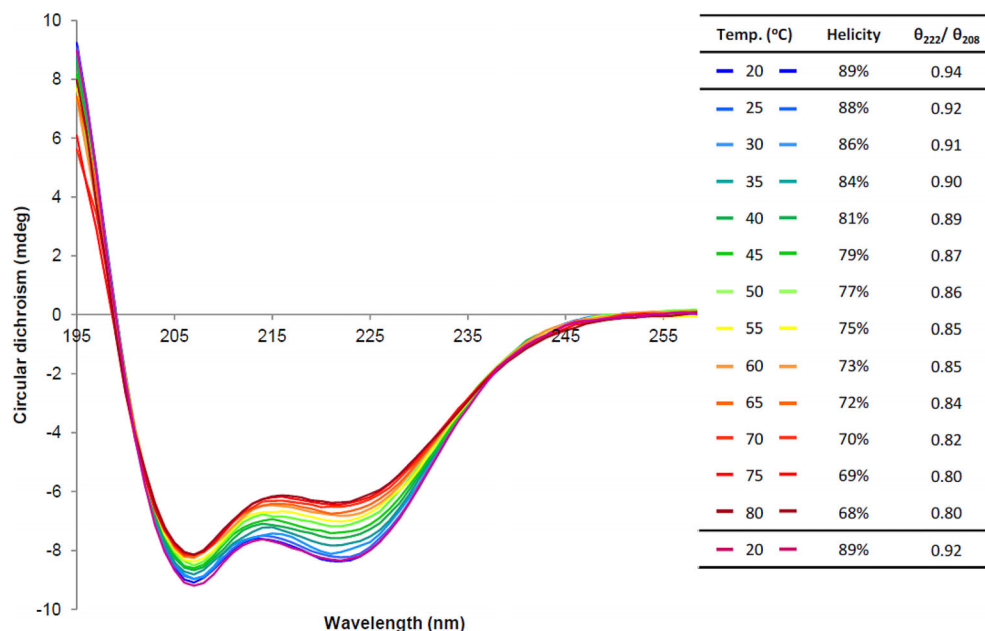
Peptides were synthesised using standard SPPS procedures adapted for hydrocarbon stapling methodology, as detailed in the materials and methods section. A total of nine peptides were synthesised in >90% purity by HPLC, including the wild type sequence of α-9 of E2-25K, and eight stapled analogues.

Following assembly by SPPS, the completed peptides were analyzed by CD spectrometry in order to determine the helical content of each staple compared to the unstabilised wild type peptide. As expected, the unstapled wild type sequence was unstructured, however all stapled analogues showed helical structures in phosphate buffer with maxima at 195 nm and dual minima at 208 and 222 nm (Figure 4). Staple 1 was shown to be remarkably ordered in solution, with a calculated helicity of 91%.
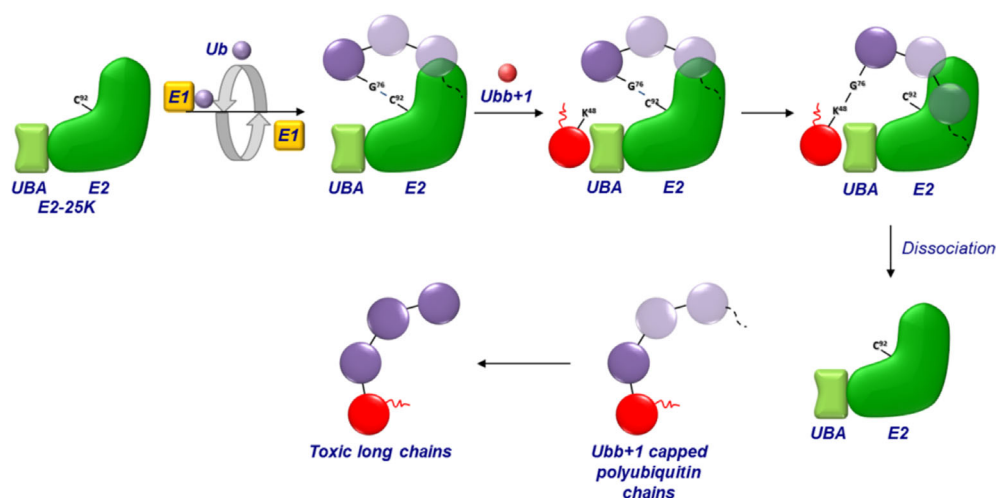
Construct 5, in which the stereochemistry of the staple is inverted compared to that of staple 1, had markedly reduced helical character (16%) which was consistent with the earlier literature findings that (R)/(R) i, i + 4 staples are in general less ordered that the (S)/(S) staples.[22] The N-terminal cyclised analogue of Staple 1, Staple 8 also had a reduced helicity of 39%, however this value was more
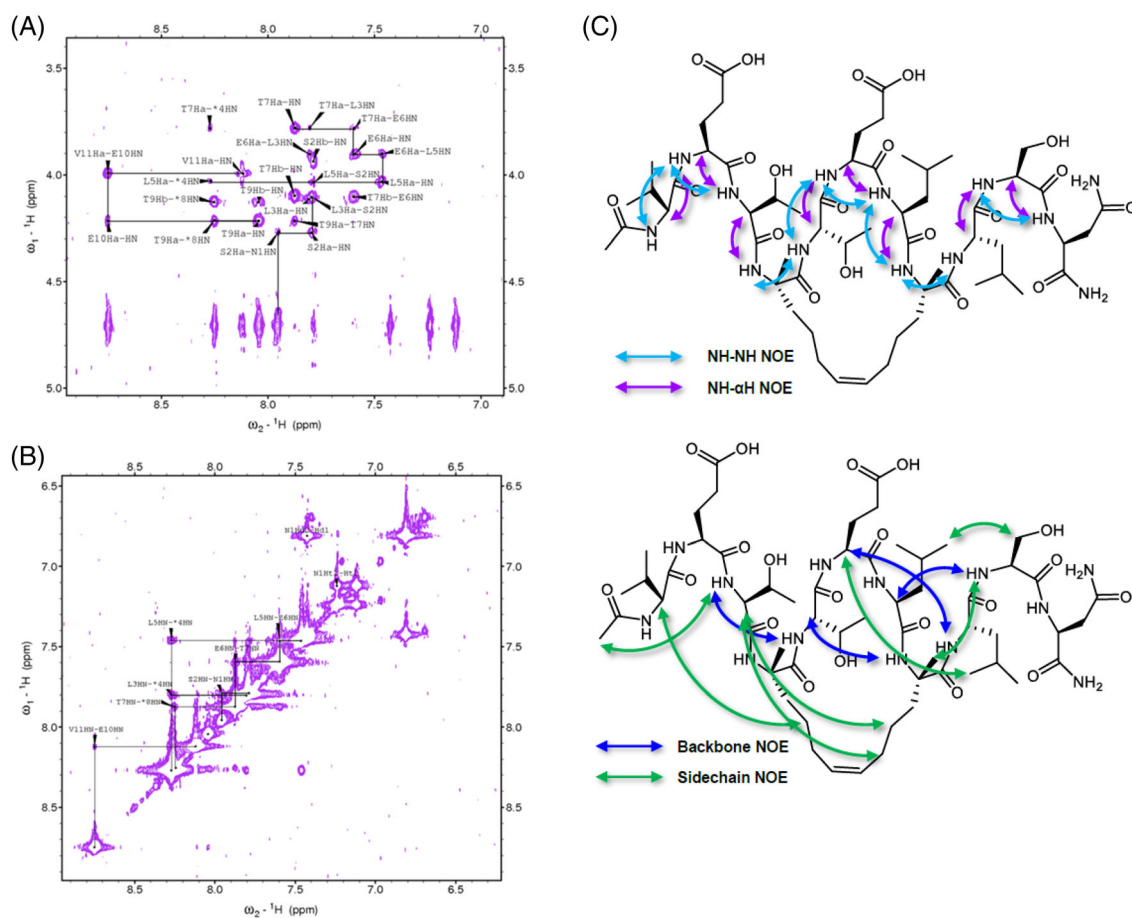


**FIGURE 5** [1]H NOESY data of staple 1. (A) Cα-NH region from the NOESY spectrum of staple 1 with two ring-closed S5 residues defined as 4* and 8*. Black lines indicate interactions between backbone amide protons and the alpha proton of the same residue (E10Ha - NH), or between a backbone NH and the alpha proton of the next residue in the sequence (V11Ha - E10NH). Longer range interactions are only possible from a coiled helical structure and indicated by yellow circles. (B) Amide NH-NH region from the NOESY spectrum of staple 1. Black lines indicate the walk along the backbone sequence (V11HN - E10HN). (C) Graphical representation of through space interactions indicating helical nature of the system

| Temp. (°C) | Helicity | $\theta_{222}/\theta_{208}$ |
|---|---|---|
| — 20 — | 89% | 0.94 |
| — 25 — | 88% | 0.92 |
| — 30 — | 86% | 0.91 |
| — 35 — | 84% | 0.90 |
| — 40 — | 81% | 0.89 |
| — 45 — | 79% | 0.87 |
| — 50 — | 77% | 0.86 |
| — 55 — | 75% | 0.85 |
| — 60 — | 73% | 0.85 |
| — 65 — | 72% | 0.84 |
| — 70 — | 70% | 0.82 |
| — 75 — | 69% | 0.80 |
| — 80 — | 68% | 0.80 |
| — 20 — | 89% | 0.92 |

**FIGURE 6** Temperature ramped CD spectra of Staple 1



**FIGURE 7** E2-25K-mediated polyubiquitin chain formation. The E2-25K conjugating enzyme (green) has two distinct binding domains. During the ubiquitination cascade, an E1 enzyme (yellow) brings a ubiquitin moiety (purple) towards the E2 binding domain of E2-25K. This Ub could itself be polyubiquitinated, provided the C-terminus is free for conjugation. An isopeptide bond is formed between the C-terminal $Gly^{76}$ of Ub and the $Cys^{96}$ of E2-25K. Ubb + 1 (red) can then bind to the UBA specific domain of E2-25K, bringing it into proximity of ubiquitin (or the growing polyubiquitin chain). A new covalent bond is formed between $Lys^{48}$ of Ubb + 1 and Gly76 of Ub giving a Ubb + 1 capped polyubiquitin chain

consistent with the other $i$, $i$ + 4 systems **2**, **3** and **6** which had helicity values of 41%, 42% and 42%, respectively. The $i$, $i$ + 7 staple examined, staple **4**, also had a very high helicity value of 80%. Lastly the isomeric helix analogue, staple **7**, had a much reduced helicity value of only 24%, indicating that amino acid sequence has a large effect on the secondary structure of these short peptides despite the all-hydrocarbon staple bridge being present.

The elevated levels of helicity exhibited by staple **1** are somewhat rare for stapled peptides, therefore a more complete structural analysis of this peptide was carried out by NMR in order to confirm the structure. $^{1}$H, NOESY and TOCSY spectra were acquired in phosphate buffer 90% $H_2O$: 10% $D_2O$, and COSY in

100% $D_2O$ allowing for complete assignment of all the residues of staple **1**.

Analysis of the NOESY spectra indicated that an α-helical structure was clearly present (Figure 5). Due to the spiral configuration of an α-helix, the NH and αH backbone protons all point parallel to one another which allows for characteristic NOE patterns. The amide NH protons all orientate towards the N-termini along with all S-amino acid side chains, while all the αH protons point towards the C-termini. Due to this conformation, an NOE walk along the backbone can be noted for each sequential NH-NH and NH-αH interaction at the $i$, and $i$ + 1 positions. In the case of staple **1**, the majority of the NH protons in the 11 amino acid sequence experienced an NOE from the preceding

**FIGURE 8** Western blot analysis of polyubiquitination assays. (A) Western blot of polyubiquitin chains. No change for any peptides against the control indirectly indicates that peptides do not bind to Ub with appreciable affintiy. (B) Western blot of Ubb + 1 capped polyubiquitin chains. Line highlighted in red shows Ubb + 1-$Ub_3$ chains. + and − indicate presence and absence of ATP (required for Ub conjugation activity, − representing control)
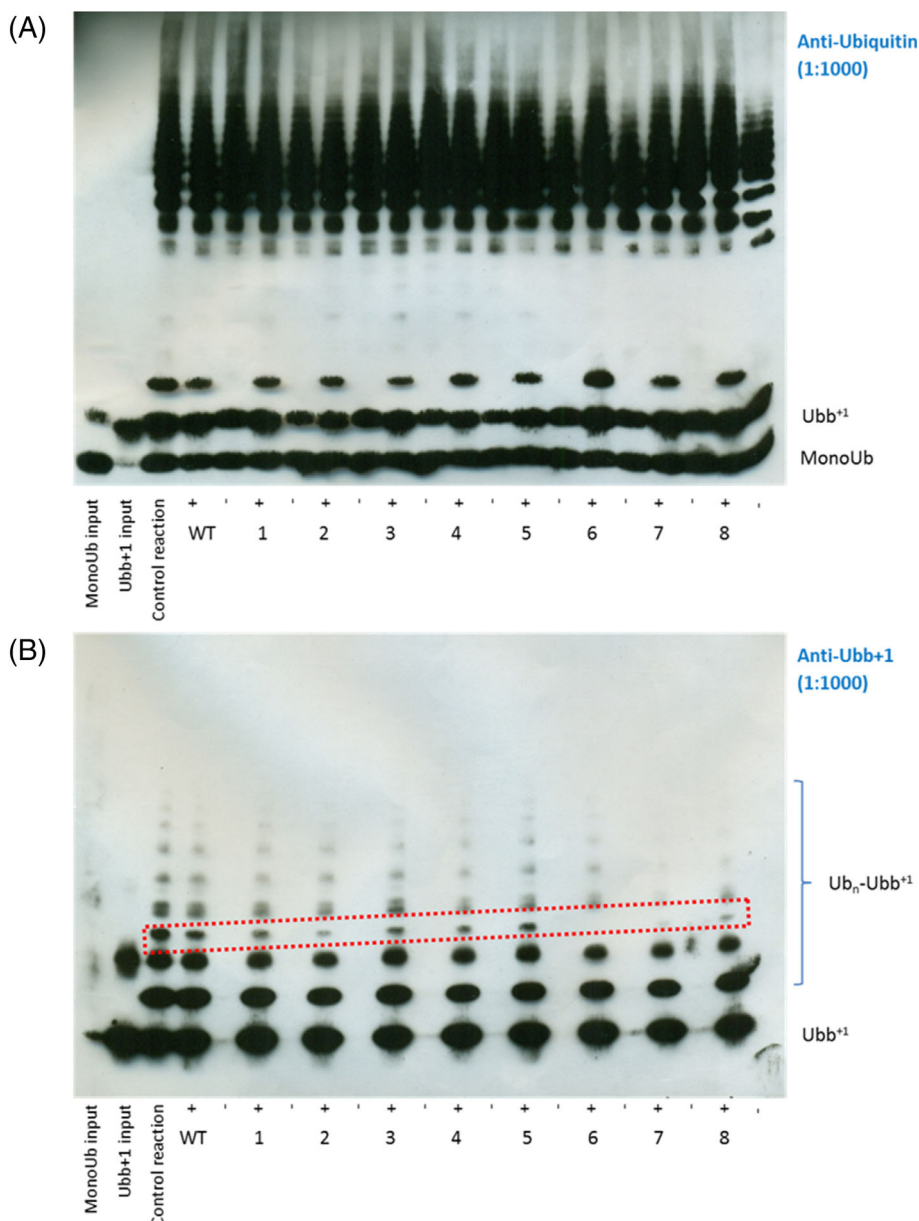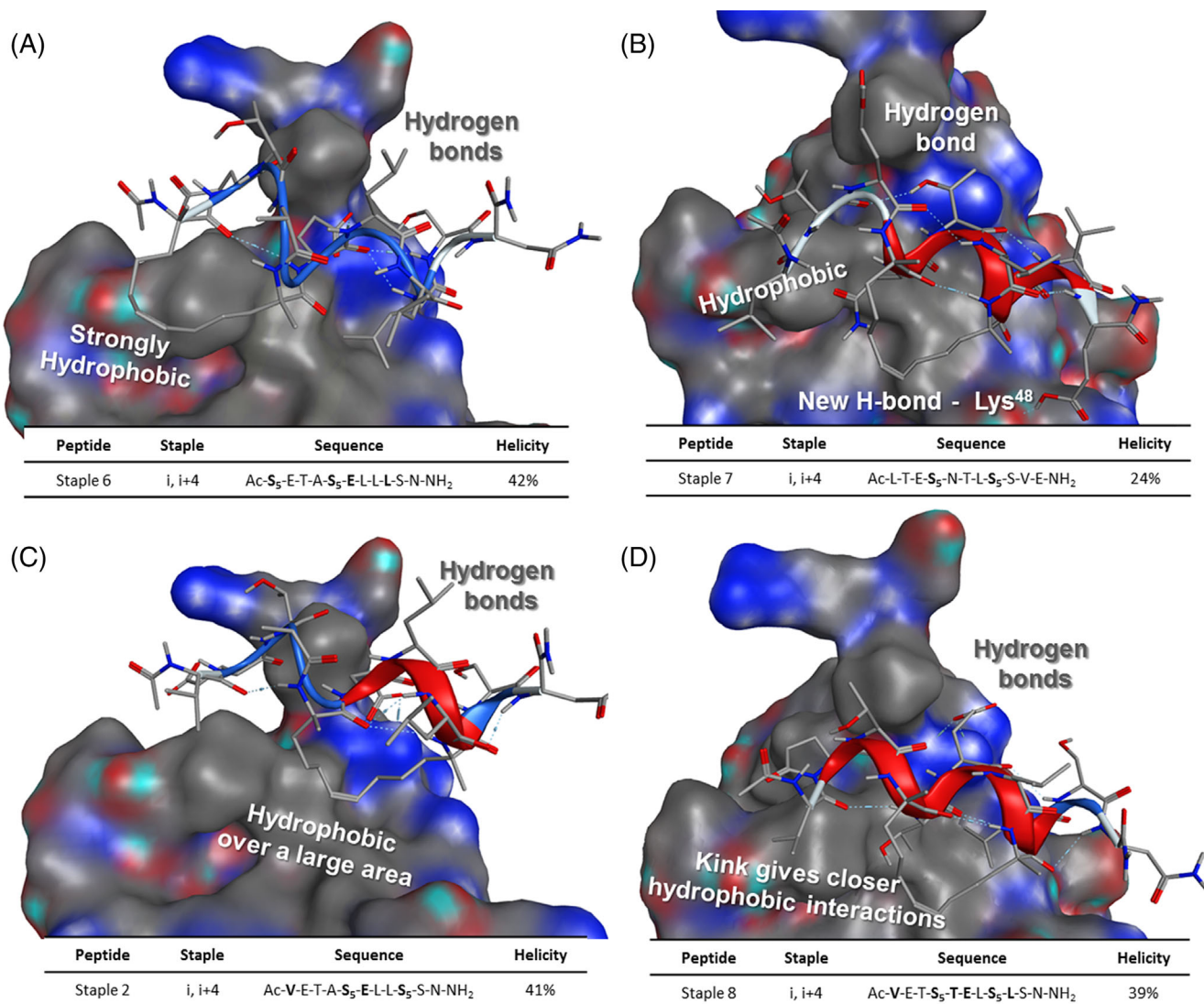


residue Similarly, all α-protons also experienced an NOE from the preceding backbone NH proton, with the exception being the S5 residues which lack an α-proton. This is strong evidence of an α-helical secondary structure as such NOE interactions would not be observed in an unstructured peptide. Full NOE data is presented in the Supporting Information.

In addition to the NMR studies of Staple **1**, it was also of interest to study the thermal stability of the constrained α-helix. This was accomplished using CD spectroscopy due to the relative ease of temperature ramping peptides in solution as well as the clear indication of helical content. In these studies it was shown that Staple **1** had significant tolerance for temperature, with helicity being maintained up to 80 °C in phosphate buffer (Figure 6). It was interesting to note that the percent helicity of Staple **1** decreased on average by 2% per 5 °C increase in temperature. At the maximum temperature tested, **Staple 1** maintained a 68% helical structure. It was also noteworthy that

upon cooling back to 20 °C, the peptide regained its highly ordered structure with the helicity returning to the original value of 89%.

Following synthesis and structural determination, the target peptides were then subjected to biological evaluation. An *in vitro* polyubiquitination assay was employed to probe the efficacy of our E2-25K peptide analogues in antagonizing the interaction between E2-25K and Ubb + 1. During E2-25K-mediated polyubiquitination, ATP facilitated ligation of Ub to an E1 enzyme via $Gly^{76}$ begins the polyubiquitination cascade. As shown in Figure 7, the single ubiquitin, or pre-formed polyubiquitin chain, is then transferred to $Cys^{98}$ of conjugating enzyme E2-25K.

The precise mechanism by which E2-25K-mediated polyubiquitination occurs is not fully defined, however it can be assumed that at this point in the polyubiquitination process, a Ub, or Ubb + 1 moiety can then non-covalently bind to the UBA domain of E2-25K.[11,12,23] At this point, the covalent link between $Lys^{48}$ of Ubb + 1 and $Gly^{76}$ of Ub

(A)

| Peptide | Staple | Sequence | Helicity |
|---------|--------|----------|----------|
| Staple 6 | i, i+4 | Ac-**S**$_5$-E-T-A-**S**$_5$-E-L-L-**L**-S-N-NH$_2$ | 42% |

(B)

| Peptide | Staple | Sequence | Helicity |
|---------|--------|----------|----------|
| Staple 7 | i, i+4 | Ac-L-T-E-**S**$_5$-N-T-L-**S**$_5$-S-V-E-NH$_2$ | 24% |

(C)

| Peptide | Staple | Sequence | Helicity |
|---------|--------|----------|----------|
| Staple 2 | i, i+4 | Ac-V-E-T-A-**S**$_5$-**E**-L-L-**S**$_5$-S-N-NH$_2$ | 41% |

(D)

| Peptide | Staple | Sequence | Helicity |
|---------|--------|----------|----------|
| Staple 8 | i, i+4 | Ac-**V**-E-T-**S**$_5$-**T**-E-L-**S**$_5$-**L**-S-N-NH$_2$ | 39% |

**FIGURE 9** Models of active peptides binding with Ubb + 1. (A) Energy minimised structure of staple 8 with Ubb + 1; (B) Energy minimised structure of staple 10 with Ubb + 1; (C) Energy minimised structure of staple 2 with Ubb + 1 and (D) Energy minimised structure of staple 11 with Ubb + 1. All models created using PDB ID:3 K90

must be formed, giving a Ubb + 1 capped polyubiquitin chain (Figure 7). As noted previously, once formed *in vivo*, these toxic Ubb + 1 capped polyubiquitin chains can impair proteasomal function which is potentially a feature of early stage AD.

As discussed previously, it was anticipated that these small peptide mimics of E2-25K would be capable of selectively binding with Ubb + 1. This would theoretically block any further interaction of Ubb + 1 with E2-25K, preventing incorporation of Ubb + 1 into polyubiquitin chains. It was reasoned that any interaction between our peptides and Ubb + 1 was likely to be weak in nature as the parent PPI between Ubb + 1 and E2-25K is also reasonably weak ($K_d$ = 0.939 ± 0.218 mM).[11] Previous study by Eom and Lee *et al.* has shown that deletion constructs of E2-25K which lack the UBA domain are capable of forming short Ubb + 1 capped polyubiquitin chains (Ub *n* = 1) suggesting the UBA domain is merely a directing group for E2-25K action, especially in facilitating longer Ubb + 1 capped polyubiquitin chains.

The polyubiquitination assay was run in duplicate for 4 h containing target peptides, E2-25K, Ub, Ubb + 1, E1 and ATP, with test peptides evaluated at 30 μM concentrations.

Analysis of the assay results from western blot analysis (Figure 8) revealed that a number of the target peptides had some efficacy in inhibiting the synthesis of longer Ubb + 1 capped polyubiquitin chains (Ub n ≥ 3) with little effect on the synthesis regular polyubiquitin chains included as a negative control. As shown above, staples **6** and **7** blocked formation of the higher order Ubb + 1-Ub$_3$ polyubiquitin chains (red box, B), whilst staples **2** and **8** had similar but more limited effects compared to controls. This readout indicated that these four peptides appeared to be selective antagonists for Ubb + 1 over Ub, blocking the longer Ubb + 1 capped polyubiquitin chains, which are generally inhibitors of the proteasome.[5,10,11,24] This apparent selectivity could be rationalised by the conformational differences between the Ub/E2-25K interaction compared to the Ubb + 1/E2-25K PPI.

The crystal structures solved by Eom and Lee *et al.* suggested a conformational tilt of 15° between Ubb + 1 with E2-25K compared to Ub, allowing for closer hydrophobic interactions with the α-9 helix of E2-25K.

A computational investigation into the possible binding modes of these peptides was then used in an effort to discern a structure activity relationship for the series. Models of the most active peptides were created from the known crystal structure of the Ubb + 1/E2-25K PPI.[11]

For the peptides associated with biological activity, molecular modelling (Figure 9) shows that the key hydrogen bond essential for binding between the peptides and $Arg^{42}$ of Ubb + 1 is maintained. In the case of staple **7**, the substitution of Glu for Thr does not appear to disrupt this interaction. For staples **6** and **2**, the hydrocarbon linker appears to interact with the hydrophobic surface of Ubb + 1. This could prove to be essential for the observed activity, as other staples (**1**, **2**, **4** and **5**) in which the linker is proposed to be solvent exposed rather than against the Ubb + 1 surface are inactive despite maintaining many other binding characteristics. The activity of staple **8** appears to be driven by similar hydrophobic interactions as the *N*-terminal cyclisation is conferring a conformational change, allowing for closer interactions with the surface of Ubb + 1, unlike the uncyclised analogue staple **1**. It was interesting to note that staple **7** appeared to be active against Ubb + 1, despite having an isomeric sequence compared to the native E2-25K. However, from consideration of the modelling data, it would appear that the C-terminal Glu of staple **8** is capable of forming a hydrogen bond with the backbone NH of $Lys^{48}$ of Ubb + 1. This could potentially occlude the key site for polyubiquitination, as $Lys^{48}$ forms the isopeptide link with $Gly^{76}$ of the growing polyubiquitin chain, hence potentially accounting for the observed biological activity.

These results are particularly interesting in that the extent of helicity of the peptide analogues of E2-25K does not appear to be a factor in determining binding affinity with Ubb + 1 as the most helical analogues, staples **1** and **4** were apparently inactive. By contrast, binding with Ubb + 1 appears to be driven by strong hydrophobic interactions, with the staple component itself potentially being beneficial with binding to our target.

## 4 | CONCLUSIONS

This work has demonstrated the feasibility of generating antagonists of the Ubb + 1/E2-25K interaction using peptide stapling methodology. A palette of peptides were successfully synthesised based on the α-9 sequence of E2-25K including the wild type sequence and eight stapled analogues with varying helicity values of 16%-91%. The exceptional level of helicity observed in staple 1 (91% in phosphate buffer) was further confirmed by NMR studies.

Four *i*, *i* + 4 stapled peptides showed varying activity against the formation of chain Ubb + 1 capped polyubiquitin chains *in vitro*. These peptides were remarkably also selective for Ubb + 1 against Ub, which could be accounted for by differences in binding modes between the two proteins. Modelling derived from the X-ray crystal structure of E2-25K in complex with Ubb + 1 was used in conjunction with biological data to offer some insight into the activities observed which is likely driven by hydrophobic interactions. Of particular interest was the interplay between the peptide helicity, staple position and target affinity with Ubb + 1 as the most structurally well-defined sequence (staple **1**) was inactive in our assay, whilst more flexible sequences in which the staple itself could participate in hydrophobic interactions with the binding surface were favoured. Overall, this study has shown that stapled helical analogues of the α-9 segment of E2-25K can selectively inhibit the formation of long chain Ubb + 1 capped polyubiquitin chains whilst maintaining regular polyubiquitination, at least *in vitro*. These tool compounds will be of further use in exploring the role of Ubb + 1 in proteasomal inhibition. Further studies in our laboratories will focus on biophysical characterisation of the interactions between this emerging class of stapled peptides and UBB + 1 (including thermal melting and ITC measurement), the design of related peptides based on biostructural considerations to improve the observed activity, and confirmation of activity in a cell-based preparation.

## ORCID

*Craig Jamieson* https://orcid.org/0000-0002-6567-8272

## REFERENCES

[1] M. S. Parihar, T. Hemnani, *J. Clin. Neurosci.* **2004**, *11*, 456.

[2] L. Martin, X. Latypova, F. Terro, *Neurochem. Int.* **2011**, *58*, 458.

[3] B. M. Riederer, G. Leuba, A. Vernay, I. M. Riederer, *Exp. Biol. Med.* **2011**, *236*, 268.

[4] S. C. Upadhya, A. N. Hegde, *BMC Biochem.* **2007**, *8*, S12.

[5] F. W. van Leeuwen, D. P. V. De Kleijn, H. H. van der Hurk, A. Neubauer, M. A. F. Sonnemans, J. A. Sluijs, S. Koycu, R. D. J. Ramdjielal, A. Salehi, G. J. M. Martens, F. G. Grosveld, J. P. H. Burbach, E. M. Hol, *Science* **1998**, *279*, 242.

[6] P. van Tijn, F. M. S. de Vrij, K. G. Schuurman, N. P. Dantuma, D. F. Fischer, F. W. van Leeuwen, E. M. Hol, *J. Cell Sci.* **2007**, *120*, 1615.

[7] D. F. Fischer, R. van Dijk, P. van Tijn, B. Hobo, M. C. Verhage, R. C. van der Schors, K. Wan Li, J. van Minnen, E. M. Hol, F. W. van Leeuwen, *Neurobiol. Aging* **2009**, *30*, 847.

[8] R. J. G. Gentier, B. M. Verheijen, M. Zamboni, M. M. A. Stroeken, D. J. H. P. Hermes, B. Küsters, H. W. M. Steinbusch, D. A. Hopkins, F. W. Van Leeuwen, *Front. Neuroanat.* **2015**, *9*, 1.

[9] Y. Lam, C. M. Pickart, A. Alban, M. Landon, C. Jamieson, R. Ramage, R. J. Mayer, R. Layfield, *Proc. Natl. Acad. Sci. U. S. A.* **2000**, *97*, 9902.

[10] L. Chadwick, L. Gentle, J. Strachan, R. Layfield, *Neuropathol. Appl. Neurobiol.* **2012**, *38*, 118.

[11] S. Ko, G. B. Kang, S. M. Song, J. Lee, D. Y. Shin, J. Yun, Y. Sheng, C. Cheong, Y. H. Jeon, Y. Jung, C. H. Arrowsmith, G. V. Avvakumov,

S. Dhe-Paganon, Y. J. Yoo, S. H. Eom, W. Lee, *J. Biol. Chem.* **2010**, *285*, 36070.

[12] R. C. Wilson, S. P. Edmondson, J. W. Flatt, K. Helms, P. D. Twigg, *Biochem. Biophys. Res. Commun.* **2011**, *405*, 662.

[13] L. Milroy, T. N. Grossmann, S. Hennig, L. Brunsveld, C. Ottmann, *Chem. Rev.* **2014**, *114*, 4695.

[14] V. Azzarito, K. Long, N. S. Murphy, A. J. Wilson, *Nat. Chem.* **2013**, *5*, 161.

[15] H. E. Blackwell, R. H. Grubbs, *Angew. Chem. Int. Ed. Engl.* **1998**, *37*, 3281.

[16] C. E. Schafmeister, J. Po, G. L. Verdine, *J. Am. Chem. Soc.* **2000**, *122*, 5891.

[17] Y. W. Kim, T. N. Grossmann, G. L. Verdine, *Nat. Protoc.* **2011**, *6*, 761.

[18] G. L. Verdine, G. J. Hilinski, *Methods Enzymol.* **2012**, *503*, 3.

[19] PureSolvMD5, http://www.solventpurification.co.uk/md (accessed: July 2014).

[20] T. D. Goddard and D. G. Kneller, https://www.cgl.ucsf.edu/home/sparky (accessed: November 2015).

[21] R. Salomon-Ferrer, D. A. Case, R. C. Walker, *WIREs Comput. Mol. Sci.* **2013**, *3*, 198.

[22] Y. W. Kim, G. L. Verdine, *Bioorg. Med. Chem. Lett.* **2009**, *19*, 2533.

[23] M. T. Haldeman, G. Xia, E. M. Kasperek, C. M. Pickart, *Biochemistry* **1997**, *36*, 10526.

[24] D. Krutauz, N. Reis, M. A. Nakasone, P. Siman, D. Zhang, D. S. Kirkpatrick, S. P. Gygi, A. Brik, D. Fushman, M. H. Glickman, *Nat. Chem. Biol.* **2014**, *10*, 664.

## SUPPORTING INFORMATION

Additional supporting information may be found online in the Supporting Information section at the end of this article.